Kinematical enhancements due to pion diffraction dissociation into $\bar{K}K^*$ and $\bar{K}^*K$: Spinless treatment

E. P. Pietiläinen† and K. E. Lassila
Ames Laboratory-ERDA and Department of Physics, Iowa State University, Ames, Iowa 50011
(Received 19 July 1976; revised manuscript received 22 February 1977)

We study pion dissociation into $\bar{K}K^*$ (or $\bar{K}^*K$) in $\pi p \to \bar{K}K^* p$ (or $\bar{K}^*Kp$) at 16-GeV/c pion momentum, finding in multiperipheral-type models that a straightforward kinematical cut can be found to isolate the K^* contribution to allow extraction of K^*N scattering information. Here we use the spinless, Berger-type, Reggeized Deck model. We find that quantitative agreement with data follows in essentially parameter-free fashion for the cross section as a function of the $K\bar{K}^*$ mass (including the sharp rise above $M_K + M_{\bar{K}^*}$), for the momentum-transfer slope dependence as a function of mass, for the partial- (angular momentum) wave amplitudes, and for the t-channel helicity-conservation characteristics of the data. The success of this straightforward approach suggests contributions of other 1^+ states coupled to the $K\bar{K}^*$ channel are not dominant effects in the $\pi p \to K\bar{K}^* p$ (or $\bar{K}K^*p$) reaction.

I. INTRODUCTION

The description of the $\rho\pi$ mass enhancement near 1.1 GeV in $\pi N \to (3\pi)N$ as a "kinematical" diffraction-dissociation effect in the context of the Regge-Deck model has become very familiar.[1] The situation with regard to the dominant diffractive process for a K-meson projectile has become more complicated since the SLAC experiment suggesting there were two resonances in the Q region.[2] It is well accepted, nevertheless, that a large diffractive contribution to the Q bump exists owing to the K dissociating into $K^*\pi$ (and also[3] $K\rho$) with subsequent rescattering of either K^* or π by the target nucleon. The resulting cross sections for such two-to-three processes are known to be large and to fall quite slowly with energy.

In this paper, we explore the diffraction of the pion into $K^*\bar{K}$ (and equivalently $\bar{K}^*K$). This should be a significant contribution to the reaction $\pi N \to (K\bar{K}\pi)N$ since the diffraction $\pi \to K^*\bar{K}$ is related to $K \to K^*\pi$ by crossing. Similar reasoning prompted us to examine pion diffraction into other heavy-mass states, such as $N\bar{N}$, $Y\bar{Y}$, and $\bar{N}\Delta$,[4] and to deduce that mass enhancements found in such pion dissociation channels can be labeled, quite reliably, as kinematic.

In Sec. II, a summary of the spinless Reggeized Deck model, as one would conventionally apply it to the $\pi p \to (K\bar{K}\pi)p$ diffractive reaction, is given. Section III contains the calculational results; in the first part the contribution of each individual diagram is presented and the last part of this section contains the results of the coherent and incoherent sums. The final section gives conclusions and further discussion of the calculated results. Inclusion of spin may modify some of the results, but the gross features of the data appear to be well explained with the spinless model, as expected from the past literature on boson diffraction.

II. THE REGGEIZED DECK MODEL

The best high-energy data relevant to the present work are on the reaction

$$\pi^+ p \to (K^+K^-\pi^+)p \tag{1}$$

at 16-GeV/c incident pion momentum.[5] For negative incident pions, inadequate data exist for detailed study but one can see qualitative similarities with experiments on reaction (1). The dominant threshold production is expected to be the pseudoscalar exchange diagram of those shown in Fig. 1. The three diagrams 1(a), 1(b), and 1(c) are very familiar in general appearance because of Ross and Yam,[6] who examined $\pi p \to \rho\pi p$ in this theoretical framework, including spin-polarization effects for the ρ. The analogous analysis for the $K\bar{K}^*$ channel has been done[7]; but here we do a detailed analysis of reaction (1) on the $K\bar{K}^*$ similar to that of Ascoli *et al.*[1] for the $\pi\rho$ system.

The charges of final-state particles in Eq. (1) limit the exchanges to K^+ and $\bar{K}^{*0}$ as shown in Figs. 1(a) and 1(b). For exchange x ($x = K$ or $\bar{K}^*$), we write the amplitude as (in subscripts, the bar will be left off the $\bar{K}^*$)

$$A_x(s, s_{KK^*}, s_p, t_\pi, t_p) = g(t_\pi)R(s_{KK^*}, \alpha_x)A^{\lambda_\xi \lambda_x}_{x\hat{p}}(s_p, t_p) \tag{2}$$

with the kinematical quantities as labeled in Fig. 1. The square of the momentum transfers from the initial-state particles are t_π and t_p; the square of the effective mass of the $K^+\bar{K}^{*0}$ system is s_{KK^*} and that for the proton with the nonperipheral meson is s_p; s is the c.m. energy squared. The subscript x denotes the Reggeized exchange parti-

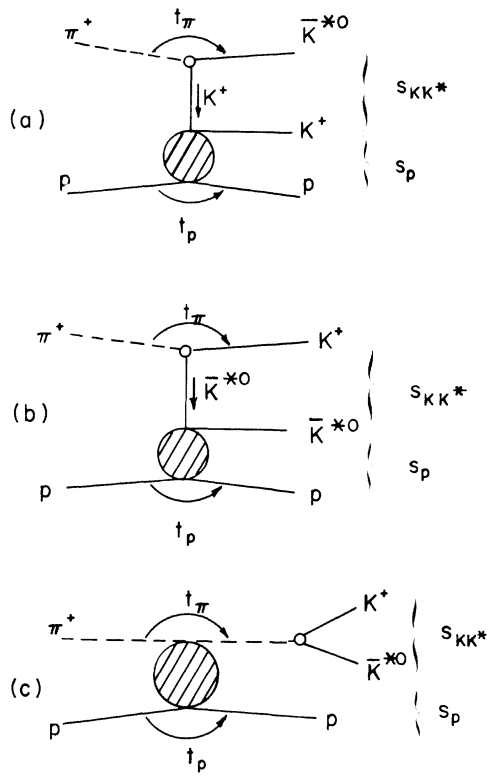

FIG. 1. Diagrams used in calculation of pion dissociation into $K^+\bar{K}^{*0}$. (a) Diagram showing π^+ dissociation into $K^+\bar{K}^{*0}$ followed by K^+p scattering. (b) Diagram for π^+ dissociation into $K^+\bar{K}^{*0}$ with subsequent $\bar{K}^{*0}p$ scattering. (c) Direct diagram for $K^+\bar{K}^{*0}$ production from a virtual pion state resulting from π^+p scattering. The momentum-transfer squared from initial to final proton is t_p; t_π is the momentum-transfer squared from the incident pion to the $\bar{K}^{*0}$ meson for diagram (a), to the K^+ meson in (b), and to the virtual pion in (c). The square of the $K^+\bar{K}^*$ subenergy is s_{KK^*} and that for the proton, adjacent meson subsystem is s_p.

cle with trajectory α_x which subsequently scatters off the proton. The amplitude for this subscattering is $A^{\lambda_x'\lambda_x}_{xp}(s_p,t_p)$, where λ_x is the helicity of the virtual exchanged particle and λ_x' its helicity after it materializes as a real particle in scattering off the proton. For $x=K$, of course, no dependence on the helicity exists. Arguments by Stodolsky[1] suggest λ and λ' will not be essential, even for questions of relative orbital angular momentum between the K and $\bar{K}^*$. The Regge-pole propagator factor is $R(s_{KK^*},\alpha_x)$. The nucleon is treated as the target for the diffractive scattering process, so its spin can be ignored. The coupling strength for $\pi^+\to\bar{K}^{*0}K^+$ along with associated kinematical factors is $g(t_\pi)$, technically to be evaluated at the off-energy shell value t_π; however, we shall use an average effective value $t_{\pi\,\mathrm{eff}}$. The on-shell decay (width Γ) $K^*\to K^+\pi^-$ as given by, e.g., Pilkuhn,[8] $\Gamma=\frac{2}{3}p^3m_{K^*}^{-2}G^2/4\pi$ fixes the coupling strength G, where p is the momentum of the K with K^* at rest. The analogous situation for $K\to K^*\pi$ coupling is treated in Ref. 9.

The amplitude for the "direct" process depicted in Fig. 1(c) is written as

$$A_\pi(s,s_{KK^*},t_\pi,t_p)=g(s_{KK^*})\frac{\exp(-as_{KK^*})}{s_{KK^*}-m_\pi^2}A_{\pi p}(s,t_p)\,, \tag{3}$$

where $A_{\pi p}(s,t_p)$ is the amplitude for π^+p elastic scattering, $g(s_{KK^*})$ is the coupling strength for $\pi^+\to\bar{K}^{*0}K^+$ including the kinematical factor $\lambda^{1/2}(s_{K\bar{K}^*},m_K^2,m_{K^*}^2)/m_{K^*}$, and the pion propagator includes a form factor with exponential slope parameter a to parametrize the effect of the rather large off-shell extrapolation. It would also include the vertex off-shell effects which are not listed separately. The function $\lambda(A,B,C)=A^2+B^2+C^2-2AB-2AC-2BC$.

The absolute value squared of the K- and K^*-exchange amplitudes from Eq. (2) are included here for completeness for the choice

$$R_{\mathrm{I}}(s_{KK^*},\alpha_x)=s_{KK^*}{}^{\alpha_x}(1+\tau e^{-i\pi\alpha_x})/\sin\pi\alpha_x\,,$$

where $\tau=\tau_x=\pm1$,

$$|A_K^{\mathrm{I}}|^2=\frac{g^2\pi^2}{2}\frac{s_{KK^*}{}^{2\alpha_K}}{1-\cos\pi\alpha_K}16\pi\lambda(s_p,m_p^2,m_K^2)B_K e^{b_K t_p} \tag{4a}$$

and

$$|A_{K^*}^{\mathrm{I}}|^2=2g^2\pi^3\frac{(\alpha_{K^*}+1)^2 s_{KK^*}{}^{2\alpha_{K^*}}}{1+\cos\pi\alpha_{K^*}}\times\lambda(s_p,m_p^2,m_{K^*}^2)B_{K^*}e^{b_{K^*}t_p}\,. \tag{4b}$$

We shall also use

$$R_{\mathrm{II}}(s_{KK^*},\alpha_x)=[\tfrac{1}{2}(s_{KK^*}-u)]^{\alpha_x}(1+\tau e^{-i\pi\alpha_x})/\sin\pi\alpha_x$$

in these expressions; u is the square of the momentum transfer from the incident pion to the K for the diagram 1(a). The K and $\bar{K}^*$ trajectories $\alpha_K(t_2)$ and $\alpha_{K^*}(t_2)=-0.24+t_\pi$ and $0.20+t_\pi$, respectively, as calculated from experimental masses and unit slope. These slopes and intercepts were not varied although leeway exists in the determinations from standard two-body reactions. The coupling $g^2\equiv g^2(t_{\pi\,\mathrm{eff}})$ is taken as $g^2=4\pi$. This is consistent with values used in the literature.[9-11] In fact, we checked the soundness of our procedure and computer code by testing against $K\to K^*\pi$ and $\pi\to\rho\pi$ diffractive calculations in Refs. 9 and 11. The plots to be presented include another isospin factor of $\frac{2}{3}$ due to the $\bar{K}^*$ decay. The absolute value squared of $A^{\lambda_x'\lambda_x}_{xp}$ in Eq. (2) summed and averaged over helicities in the intermediate state scat-

tering leads to the remaining factor in Eqs. (4a) and (4b) (this assumption has been studied[7]); $b_K(b_{K^*})$ and $B_K(B_{K^*})$ are the slopes and normalizations, respectively, for the $K^+p(\bar{K}^*p)$ elastic (Pomeron exchange) scattering subprocess. The relevant values for K^+p scattering are taken from data, e.g., with

$$b_K = 1.25 + 1.98 \ln(s_p/2.04) \tag{5}$$

which very satisfactorily reproduces the energy dependence of the K^+p slope.[12] The forward elastic cross section $d\sigma/dt\big|_{t'=0}$ determines B, and the results are essentially unaffected if $B = \sigma_{\text{tot}}{}^2/16\pi$ with $\sigma_{\text{tot}}(K^+p) = 17$ mb. For $\bar{K}^*p$ scattering we approximate these parameters to zeroth order to be the same as those for K^-p scattering since in the quark model the same strange-antiquark–proton scattering is involved in both. Therefore, we have taken $b_{K^*} = 7.0$ with B_{K^*} given by $\sigma_{\text{tot}}(\bar{K}^*p) = 22$ mb. We found that these approximations led to an adequate representation of $|A_{xp}(s_p, t_p)|^2$. Finally, the low mass side of s_p was cut off for values less than 3 GeV^2. Since three- or four-body phase space causes the contribution to vanish for s_p near threshold, an insignificant contribution has been neglected to save doing the complete low-energy parametrization. The effect was studied in detail, and test calculations compared excellently with results in recent related[11] calculations.

III. CALCULATIONAL RESULTS

To apply the Regge-Deck formulas discussed in the previous section, it is useful to first develop some feeling for the relative contributions of the individual diagrams in Fig. 1. Therefore, Sec. III A is devoted to examining these contributions separately. Sec. III B contains results following from combining the amplitudes coherently and incoherently, along with relevant data comparisons.

A. Separate contributions of diagrams

Predictions following from the model can now be compared with data. Monte Carlo techniques incorporating important sampling procedures[13] were used to produce the distributions to be discussed. The $K\bar{K}^*$ effective-mass distribution predicted for $R_{\text{II}} \propto [\frac{1}{2}(s_{K\bar{K}^*} - u)]^\alpha$ from each of the separate diagrams of Fig. 1 is shown in Fig. 2. Near threshold the largest contribution comes from K exchange (solid curve) which is about twice as big as $\bar{K}^*$ exchange (dashed curve) at $s_{K\bar{K}^*} = 2.2$ GeV^2. The dot-dash curve shows the distribution given by the direct term of Fig. 1(c) for two form factors in Eq. (3), the higher curve following from $a = \frac{3}{4}$ and the lower-lying curve from $a = 1.0$. With these form factors, the direct diagram contribution is

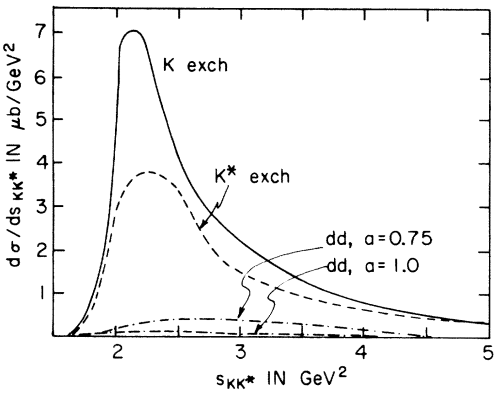

FIG. 2. Effective-mass contributions of diagrams in Fig. 1. The solid line gives the $s_{K\bar{K}^*}$ distribution due to K exchange, $|A_K^{\text{II}}|^2$, the dashed line correspondingly is due to K^* exchange, $|A_K^{\text{II}*}|^2$, and dot-dash lines are due to the direct diagram (dd), Fig. 1(c), for form factors given by $a = \frac{3}{4}$ and 1.

quite negligible compared with the K- and $\bar{K}^*$-exchange contributions. It is reasonably well known that such direct-channel pole terms require some kind of damping factors since the tails of these amplitudes lead to deeper theoretical difficulties.[14]

Of the many possible distributions we might display, those which could enable one to isolate a particular diagram are of most interest. The polar and azimuthal angle distributions in the $K\bar{K}^*$ rest frame for the K- and $\bar{K}^*$-exchange diagrams are shown in Figs. 3 and 4 for R_{II} in Eq. (2). The portion labeled (a) in each figure shows these angular distributions in the Gottfried-Jackson (GJ) frame where the z axis is given by the incident pion direction. In this frame θ_{GJ} is the polar angle between the z axis and the $\bar{K}^*$ momentum and $\phi \equiv \phi_{\text{TY}}$ (Treiman-Yang angle) is the azimuthal angle measured from the production plane, the normal to this plane being in the direction of $\hat{z} \times \vec{p}_{p\,\text{out}}$. The lower (b) part of Figs. 3 and 4 shows the distributions in the s-channel helicity frame (SCHF) for which the polar angle is measured from the z axis along the outgoing proton momentum and the azimuthal angle measured from the production plane (the normal being in the direction of $\vec{p}_{\pi\,\text{inc}} \times \hat{z}$). The pronounced peaking of the distributions in $\cos\theta_{\text{GJ}}$ is made logical by considering the dynamical differences between the diagrams of Figs. 1(a) and 1(b). For K exchange, the $\bar{K}^*$ dominantly continues along the incident-pion momentum while for the $\bar{K}^*$-exchange diagram, the K continues predominantly forward with the $\bar{K}^*$ therefore going backward. If the $\bar{K}^*$ distribution is measured relative to the final proton direction the obvious correlations with the incident pion get washed out considerably.

The ϕ distributions in Fig. 4 can be understood similarly; for, if the $\overline{K}^*$ tends to go along or opposite to the incident-pion direction there can be little variation as the azimuthal angle ϕ_{TY} is changed. On the other hand, if the z axis is defined differently, as along the out-going-proton momentum, the strong correlation of the $\overline{K}^*$ with the incident pion noted in Fig. 3(a) as a function of $\cos\theta_{GJ}$ will be reflected in this new azimuthal dependence [as for ϕ_H in Fig. 4(b)].

From Figs. 3 and 4, it is clear that with cuts in $\cos\theta_{GJ}$ and/or ϕ_H one can most effectively enhance the K- or $\overline{K}^*$-exchange diagrams. Similar suggestions have been made for enhancing K^* exchange in the Q region or ρ exchange in the A_1 region.[11] However, one notes that background under the peak due to the other exchange is not eliminated totally. Additionally, the direct diagram, Fig. 1(c), contributes a constant though small amount to both these angular distributions.

We find a kinematical cut with which to isolate at least part of the $\overline{K}^*$-exchange diagram relatively cleanly. A plot of $d\sigma/ds_{pK^*}$ vs s_{pK^*}, where s_{pK^*} is the effective mass squared of the $\overline{K}^*$-p system, for the K-exchange and $\overline{K}^*$- exchange diagrams, is shown in Fig. 5. The direct diagram, Fig. 1(c), contribution is also shown for $a=\frac{3}{4}$; this is small and similar to that due to K exchange. Therefore, requiring that s_{pK^*} be less than ~13 GeV^2 isolates a very clean segment of the $\overline{K}^*$-exchange contribution. The lower limit need not be $m_p+m_{K^*}$. An experimental approach could therefore use this type of cut to obtain information on the $\overline{K}^*p$ inter-

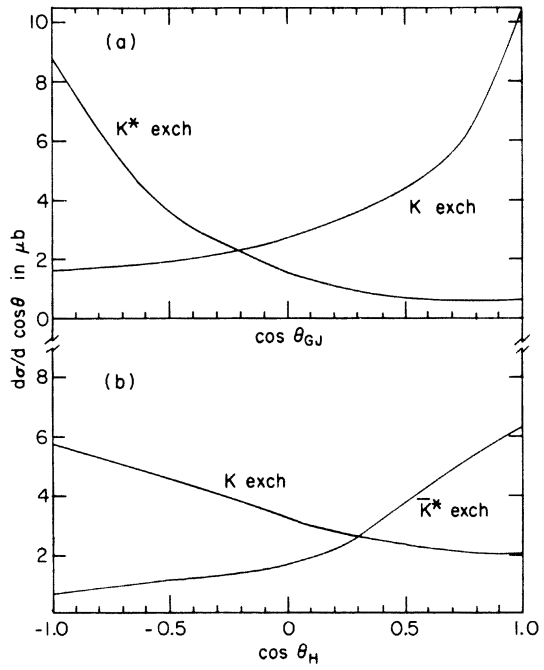

FIG. 3. Distributions in $\cos\theta_{KK^*}$ in the $(K\overline{K}^*)$ rest system for the K- and $\overline{K}^*$-exchange diagrams calculated for (a) $\theta_{KK^*}=\theta_{GJ}$, the polar angle in the Gottfried-Jackson frame and (b) $\theta_{KK^*}=\theta_H$, the polar angle in the s-channel helicity frame. In the $K\overline{K}^*$ rest frame, the $\overline{K}^*$ is moving along the incident-pion momentum direction when $\cos\theta_{GJ}=1$ and opposite to the outgoing proton when $\cos\theta_H=1$. The distributions due to the direct diagram are not shown as they are constant.

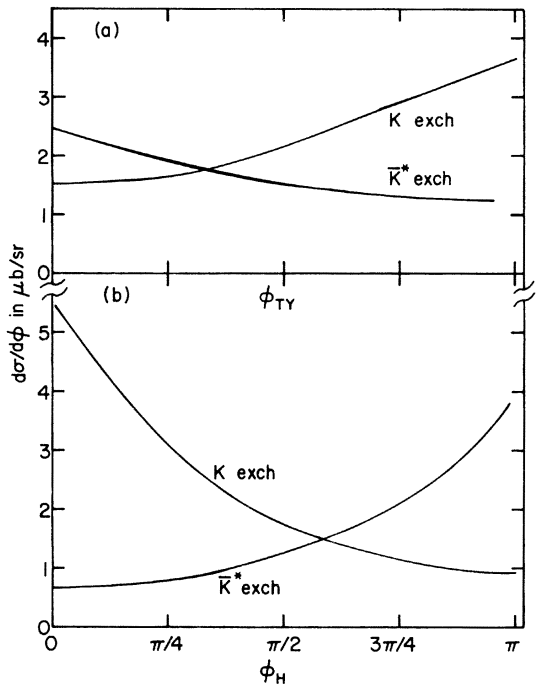

FIG. 4. Distributions in the azimuthal angle ϕ_{KK^*} in the $(K\overline{K}^*)$ rest system for the K- and $\overline{K}^*$-exchange diagrams calculated for (a) $\phi_{KK^*}=\phi_{TY}$, the Trieman-Yang angle or the azimuthal angle in the Gottfried-Jackson frame and (b) $\phi_{KK^*}=\phi_H$, the azimuthal angle in the s-channel helicity frame.

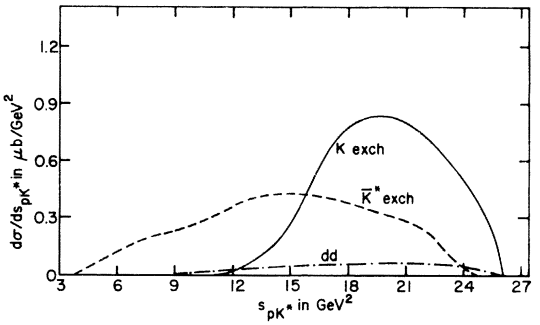

FIG. 5. Distributions in effective mass squared for the $\overline{K}^*p$ system for the (solid line) K-exchange contribution $|A_K^{II}|^2$, the (dashed line) $\overline{K}^*$-exchange contribution $|A_{K^*}^{II}|^2$, and (dot-dash line) for the direct diagram of Fig. 1(c) with $a=0.75$.

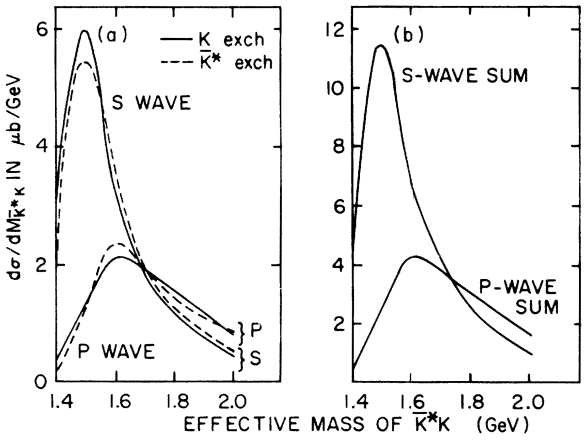

FIG. 6. Results of performing partial-wave projections on the diagrams shown in Figs. 1(a) and 1(b). (a) Absolute values squared of $\bar{K}^*K$ S- and P-wave amplitudes given by each of the K-exchange and $\bar{K}^*$-exchange diagrams in the t-channel helicity frame. (b) Sum of the S-wave cross section from K exchange and S-wave cross section due to K^* exchange. The analogous curve for the P wave is also shown. The amplitudes projected are A^{I}_K and $A^{\mathrm{I}}_{K^*}$.

action directly without the necessity for assuming it to be the same as K^-p scattering.

A very interesting question concerns the partial-wave content of the $\bar{K}^*K$ system. The phase-signature factor of the Regge propagator in Eq. (2) must explicitly be included (i.e., $1 \pm e^{i\pi\alpha_x}$ with + going with $x = K$) before angular momentum states of $\bar{K}^*K$ are projected out. Since the conventional Regge-Deck amplitudes as given in Eq. (2) ignore the spins of the external particles, it is sufficient to project this amplitude in the $\bar{K}^*K$ rest frame upon $Y_{\mathrm{LM}}(\theta, \phi)$. In the t-channel helicity (TCH) or Gottfried-Jackson frame these spherical angles θ, ϕ are just the $\theta_{\mathrm{GJ}}, \phi_{\mathrm{TY}}$ discussed above. The absolute squared amounts of $L = 0$ and $L = 1$ wave calculated with $R_{\mathrm{I}} \propto s^{\alpha_x}$ in the K-exchange diagram (solid line) and K^*-exchange diagram (dashed line) are shown in Fig. 6(a) in the TCH frame. We find for both diagrams that the contribution from $M = \pm 1$ is very small. In the SCHF, the contribution from $M = \pm 1$ states is no longer negligible, since it is more than an order of magnitude larger than that in the TCH frame. Thus, the statement is made that these diagrams obey TCH conservation in the conventional Regge-Deck model, an observation expected from the early work of Stodolsky to be independent of K^* spin.

Finally, before studying combined $\bar{K}^*$- and K-exchange amplitudes, it is of interest to get some feel for the net, separate amount of S or P waves possible from these diagrams. In Fig. 6(b), the absolute value squared of the S-wave amplitude due to K exchange is added to that due to $\bar{K}^*$ exchange, and similarly for the P wave. The expected dominance of the S wave is seen.

B. Combined contributions

The amplitudes for the three diagrams in Fig. 1 should be combined coherently if each diagram contributes independently to the $K^+K^-\pi^-$ final state in the same region of phase space. As seen from Figs. 3, 4, and 5 in some kinematic variables, there are regions where the contributions overlap little, and considerable incoherence between the amplitudes exists. We therefore present results for both coherent and incoherent sums of these amplitudes. The finer details of the coherent-addition results are expected to be modified somewhat when the K^* spin is correctly treated. However, the data are still in the primitive stages so the main features presented are well described by the model as we expect from Stodolsky's[1] arguments; for example, we are not too surprised that most of the $K\bar{K}^*$ relative angular momentum predictions are reasonable. [Possibly from the deeper purely theoretical point of view one might hope that the incoherent sum would be adequate, indicating relatively little overlap between the dominant amplitudes, as the diagrams of Figs. 1(a) and 1(b) might to be parts of one dual amplitude.]

The threshold behavior predicted by the onset of $K\bar{K}^*$ diffraction of the pion is compared with data for $\pi^+p \to K^+K^-\pi^+p$ in Fig. 7. The curves represent

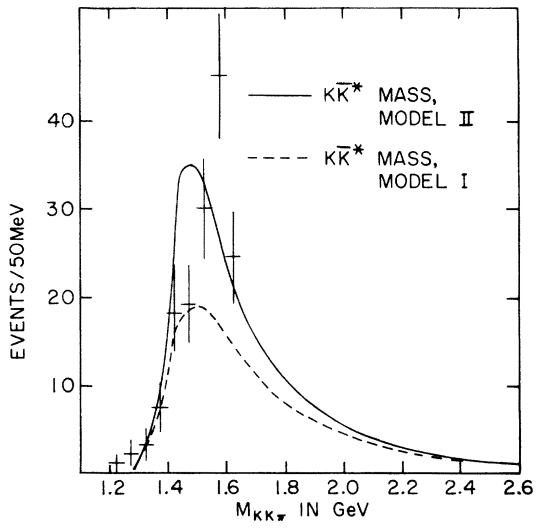

FIG. 7. Comparison of the raw $K^+K^-\pi^+$ data at 16 GeV/c in $\pi^+p \to (K^+K^-\pi^+)p$ with calculation for $\bar{K}^*K$ production. The solid line is calculated with the Regge propagator $R_{\mathrm{II}} \propto [\frac{1}{2}(s_{K\bar{K}^*} - u)]^{\alpha}$ and the dashed curve with $R_{\mathrm{I}} \propto s^{\alpha}_{K\bar{K}^*}$. The K- and $\bar{K}^*$-exchange terms are added incoherently.

TABLE I. Values of the slope parameter b_+ in GeV^{-2} for coherent and incoherent sums of K- and K^*-exchange amplitudes for cases I and II (Regge propagators $\propto s^\alpha$ and $[\frac{1}{2}(s-u)]^\alpha$, respectively); b_+ is the slope parameter in $d\sigma/dt_p \propto \exp(b_+ t_p)$, where t_p is equivalent to the momentum transfer squared from the incident π^+ to the $(K^+K^-\pi^+)$ system. The error in the numbers given by theory is 5% for the most uncertain determination but typically it is 3%.

$\pi^+K^-K^+$ mass bin		1.4–1.8 GeV	1.8–2.2 GeV
Experiment (Ref. 5)		7.3 ± 0.7	5.5 ± 0.7
Theory			
Case I	$\lvert A_K\rvert^2 + \lvert A_{\bar{K}^*}\rvert^2$	6.4	4.9
	$\lvert A_K + A_{\bar{K}^*}\rvert^2$	6.8	5.1
Case II	$\lvert A_K\rvert^2 + \lvert A_{\bar{K}^*}\rvert^2$	6.2	5.1
	$\lvert A_K + A_{\bar{K}^*}\rvert^2$	7.2	5.3

TABLE II Values of the slope parameter b_- in GeV^{-2} for coherent and incoherent sums of K- and $\bar{K}^*$-exchange amplitudes for cases I and II (Regge propagators $\propto s^\alpha$ and $[\frac{1}{2}(s-u)]^\alpha$, respectively). This slope parameter for $\pi^-p \to (K^*K^-)p$ is to be compared with that of Table I for the $\pi^+p \to (\bar{K}^*K^+)p$ reaction.

$\pi^-K^-K^+$ mass bin		1.4–1.8 GeV	1.8–2.2 GeV
Experiment (Ref. 5)		8.7 ± 1.1	5.6 ± 1.2
Theory			
Case I	$\lvert A_{K^-}\rvert^2 + \lvert A_{K^{*0}}\rvert^2$	7.5	5.4
	$\lvert A_{K^-} + A_{K^{*0}}\rvert^2$	7.8	5.5
Case II	$\lvert A_{K^-}\rvert^2 + \lvert A_{K^{*0}}\rvert^2$	8.1	5.7
	$\lvert A_{K^-} + A_{K^{*0}}\rvert^2$	8.6	5.7

the incoherent sums of K- and $\bar{K}^*$-exchange amplitudes with Regge propagators $R_{\rm I} \propto s_{KK^*}^{\alpha_K}$ (dashed curve) and $R_{\rm II} \propto [\frac{1}{2}(s_{KK^*} - u)]^{\alpha_K}$ (solid line). The data shown are explicitly for the $K^+K^-\pi^+$ effective mass without requiring that the K^- and π^+ make the $\bar{K}^*(890)$ resonance. The threshold for $K^+K^-\pi^+$ production is at 1.08 GeV. The data show a dramatic increase only near $M_{K^+K^-\pi^+} = 1.4$ GeV, which is the $\bar{K}^*K$ threshold (smeared appropriately according to the $\bar{K}^*$ width). This is similar to the 3π mass spectrum in the reaction $\pi p \to (3\pi)p$ where a dramatic increase occurs above the $\rho\pi$ threshold. This threshold behavior is essentially unchanged when the coherent sum is taken. Before comparing the present calculations with the partial-wave projection of $\bar{K}^*K$ states from $K\bar{K}\pi$ data, we examine the dependence on the t_1 momentum transfer squared variable.

The prediction of the t_p slope decreasing with increasing s_{KK^*} also agrees with experiment. That the slopes tend to be larger for incident negatively charged pions is well explained in the model. The dominant diagram in π^- diffraction has K^- exchange and the K^-p part of the amplitude exhibits a sharper diffractive peak than does the K^+p amplitude used in π^+ diffraction. The slope parameter values for cases I and II (Regge propagator with s^α and $[\frac{1}{2}(s-u)]^\alpha$, respectively) for incoherent and coherent K^+- and $\bar{K}^{*0}$- exchange amplitudes in π^+ diffraction are listed in Table I. We note that the amplitudes A_{K^+} and $A_{\bar{K}^{*0}}$ tend to contribute to different s_{Kp} regions as $K\bar{K}^*$ mass increases, so little difference is seen between the coherent and incoherent calculations of the theory slopes in the high-mass bin. However, in the peak region the coherent sum, with phases given by conventional Regge-pole theory gives a slope in very good agreement with experiment. The incoherent sum of amplitudes predicts slope values which compare *adequately* with the data, though perhaps somewhat low. For the incident π^- diffracting into K^*K^-, Table II shows the similar comparison between experiment and calculated slopes. Again the model (which now has K^--exchange and K^*-exchange diagrams) produces good agreement with slope measurements.

Since the model calculation predicts the threshold behavior and the t_p dependence so well, it appears useful now to turn to more stringent tests possible by comparing with the $\bar{K}^*K$ portion of the partial-wave, or modified Ascoli analysis,[15] of the $K\bar{K}\pi$ system. The partial-wave content of the individual K- and $\bar{K}^*$-exchange graphs was studied at the end of part A of this section. It was seen that the absolute amounts of S wave from each diagram dominated over the other partial waves but the P-wave contribution was important in the tail

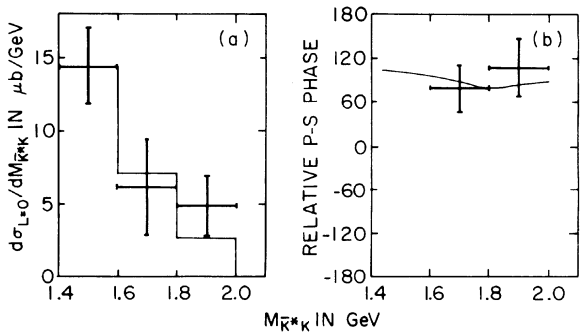

FIG. 8. Plots of (a) the $\bar{K}^*K$ $L=0$ partial cross section and (b) the relative P wave to S wave phase versus $m_{\bar{K}^*K} = (s_{K^*K})^{1/2}$ (the $\bar{K}^*K$ effective mass) calculated for the sum (coherent) of the K- and $\bar{K}^*$-exchange amplitudes, $A_K^{\rm I} + A_{\bar{K}^*}^{\rm I}$, with Regge propagator $R_{\rm I} \propto s^\alpha$.

region beyond $s_{K^*K}^{1/2} = 1.6$ GeV. When the K- and $\bar{K}^*$-exchange amplitudes are added coherently, interference within a given angular momentum state might change the results from those in Fig. 6. The final figure, Fig. 8, shows the $L = 0$ component of this coherent sum calculated with the Regge propagator $R_I \propto s^{\alpha_x}$ compared with data. The data are explicitly for the relative $l = 0$, $\bar{K}^*K$ state produced in $\pi^+p \to K^+K^-\pi^+p$ at 16-GeV/c incident pion momentum, as given by Seyfert.[16] Our earlier analysis[4] of this reaction was done from the information given in Ref. 5 in which only the combined cross sections for $\pi^+p \to K^+K^-\pi^+p$ and $\pi^-p \to K^+K^-\pi^-p$ were given. Insufficient information was available to allow the separation of reactions. The combined data were therefore used earlier since the $K^+K^-\pi^-$ fraction was stated as a small fraction and the $\pi^+p \to K^+K^-\pi^+p$ data "gave results very similar to those of the combined data".[5]

As seen in Fig. 8(a) the S-wave content of $A_K^I + A_{\bar{K}^*}^I$ (the I superscript means R_I is used) with no fitted parameters is in excellent agreement with the $L = 0$, $\bar{K}^*K$ data. Further, the same statement applies to the relative phase between the P-wave and S-wave $\bar{K}^*K$ partial waves plotted in Fig. 8(b) as a function of mass—though the data are somewhat limited. From this relative phase data one can argue strongly for the presence of *both* K and $\bar{K}^*$ exchange. For pure K exchange this relative phase is negative; for $\bar{K}^*$ exchange, it is about twice as large as the data. Also, the data for $d\sigma^{L=0}/dM_{KK^*}$ in Fig. 8 can be compared with the incoherent addition of S-wave contributions in Fig. 6. Either K or K^* exchange by itself is inadequate.

Using the Regge propagator $R_{II} \propto [\frac{1}{2}(s_{KK^*} - u)]^{\alpha_x}$ instead of R_I in these comparisons causes little change in the relative P-S phase, but does produce a cross section in the first bin, 1.4–1.6 GeV, in Fig. 8(a) of 24.6 μb/GeV. Further comparisons can be made from Tables III and IV where the $\bar{K}^*K$ S- and P-wave partial cross sections for various possible theoretical calculations are listed. We note that the experiment[16] found no P wave at $s_{K^*K}^{1/2} = 1.5 \pm 0.1$ GeV, but at 1.7 ± 0.1 GeV this cross section is 10.3 ± 3.4 μb/GeV. At $s_{K^*K}^{1/2} = 1.9 \pm 0.1$ GeV it has fallen to 2.1 ± 2.3 μb/GeV. The high value at $s_{K^*K}^{1/2} = 1.7$ GeV drops to 9 ± 3.6 μb/GeV in the analysis[5] with the $K^+K^-\pi^+$ and $K^+K^-\pi^-$ data combined. Therefore, it can be concluded that a higher-statistics experiment is needed to pin down the amount of the P wave. Nevertheless, the possibility for a considerable P-wave cross section does exist in the model. This is seen by noting that in the middle bin pure K exchange gives 2.47 μb/GeV and K^* exchange gives 2.00 μb/GeV. If the two diagrams were in phase, the cross section would be 8.9 μb/GeV. But we see from Tables III and IV that the Regge rotating phases are such as to cause considerable P-wave cancellation.

Calculations involving partial waves and coherence of amplitudes are expected to be the most sensitive to correct use of $\bar{K}^*$ spin and helicity states. However, our above comparisons concerned relative angular momentum states between the K and $\bar{K}^*$ and not the $\bar{K}^*$ helicity directly. Also supporting the view that the general features are not seriously affected is the fact that the K- and $\bar{K}^*$-exchange amplitudes are intrinsically "quite" incoherent; as seen from Figs. 3, 4, and 5, the differences in contribution are not directly concerned with $\bar{K}^*$ helicities. Too, the cancellation

TABLE III. Tabulation of angular-momentum-zero ($L = 0$) cross section in μb/GeV for production of the $\bar{K}^*K$ system in three mass bins between 1.4 and 2.0 GeV. The subscript K or K^* refers to the K- or K^*-exchange diagram and the superscript I or II refers to s^α or $[\frac{1}{2}(s_{KK^*} - u)]^\alpha$ in the Regge propagator.

$\bar{K}^*K$ mass bin	1.4–1.6 GeV	1.6–1.8 GeV	1.8–2.0 GeV
Experiment ($L = 0$)	14.4 ± 2.6	6.2 ± 3.3	4.8 ± 2.1
$\lvert A_K^{I,L=0}\rvert^2$	4.4	2.0	0.8
$\lvert A_{K^*}^{I,L=0}\rvert^2$	4.0	2.2	0.8
$\lvert A_K^{I,L=0}\rvert^2 + \lvert A_{K^*}^{I,L=0}\rvert^2$	8.4	4.2	1.6
$\lvert A_K^{I,L=0} + A_{K^*}^{I,L=0}\rvert^2$	14.3	7.1	2.7
$\lvert A_K^{II,L=0}\rvert^2$	9.1	3.5	1.2
$\lvert A_{K^*}^{II,L=0}\rvert^2$	5.5	2.7	0.9
$\lvert A_K^{II,L=0}\rvert^2 + \lvert A_{K^*}^{II,L=0}\rvert^2$	14.5	6.2	2.1
$\lvert A_K^{II,L=0} + A_{K^*}^{II,L=0}\rvert^2$	24.7	10.5	3.5

TABLE IV. Tabulation of angular-momentum-one ($L=1$) cross section in μb/GeV for production of the $\bar{K}^*K$ system in three mass bins between 1.4 and 2.0 GeV. The subscript K or K^* refers to the K- or K^*-exchange diagram and the superscript I or II refers to s^α or $[\frac{1}{2}(s_{KK^*}-u)]^\alpha$ in the Regge propagator.

$\bar{K}^*K$ mass bin	1.4–1.6 GeV	1.6–1.8 GeV	1.8–2.0 GeV
Experiment ($L=1$)	···	10.3 ± 3.4	2.1 ± 2.3
$\lvert A_K^{\mathrm{I},L=1}\rvert^2$	1.2	1.7	1.2
$\lvert A_{K^*}^{\mathrm{I},L=1}\rvert^2$	1.2	1.9	1.1
$\lvert A_K^{\mathrm{I},L=1}\rvert^2+\lvert A_{K^*}^{\mathrm{I},L=1}\rvert^2$	2.4	3.6	2.3
$\lvert A_K^{\mathrm{I},L=1}+\lvert A_{K^*}^{\mathrm{I},L=1}\rvert^2$	0.9	1.2	0.8
$\lvert A_K^{\mathrm{II},L=1}\rvert^2$	1.7	2.5	1.6
$\lvert A_{K^*}^{\mathrm{II},L=1}\rvert^2$	2.5	2.0	1.2
$\lvert A_K^{\mathrm{II},L=1}\rvert^2+\lvert A_{K^*}^{\mathrm{II},L=1}\rvert^2$	4.2	4.5	2.8
$\lvert A_K^{\mathrm{II},L=1}+A_{K^*}^{\mathrm{II},L=1}\rvert^2$	1.4	1.5	1.0

shown for π and p exchange in the A_1 region by Stodolsky[1] likewise did not depend on the ρ helicity.

Finally, the calculations with coherent K- and $\bar{K}^*$-exchange amplitudes can be performed in the s-channel helicity frame. (The z axis is defined by the outgoing proton.) For amplitudes given by $R_{\mathrm{I}}\propto s^{\alpha_K}$ we find the ratio of the cross section with $M=\pm1$ ($L=1$, of course) in the SCHF to that in the TCHF to be 5.1 at the peak or averaged between $s_{KK^*}^{1/2}=1.4$ and 2.0 GeV. For $R_{\mathrm{II}}\propto[\frac{1}{2}(s_{KK^*}-u)]^{\alpha_K}$, this ratio is 4.5. As noted in part A of this section, the individual diagrams gave ~12 for this ratio.

IV. DISCUSSION AND CONCLUSIONS

To the best of our knowledge, our work is the first to consider pion diffraction dissociation into $K\bar{K}^*$ (or $K^*\bar{K}$). We anticipated that such a process as $\pi\to K\bar{K}^*$ with subsequent rescattering of the K or $\bar{K}^*$ on the target nucleon to produce an enhancement in the effective mass of the $K\bar{K}^*$ system must exist. A dominant process in K-meson reactions has the K diffracting into $K^*\pi$ to produce (at least a large part of) the Q bump, which is related to the present $\pi\to K\bar{K}^*$ reaction simply by crossing. An experiment[5] published in 1975 which had not been previously theoretically analyzed turned out to provide a good testing ground for these ideas which we pursued here in a spinless model appropriate for first calculations.

The present treatment of $\pi\to K\bar{K}^*$ (or $\bar{K}K^*$) in the Reggeized Deck model gave a good explanation for essentially all aspects of these data. The rise in the $K\bar{K}\pi$ production cross section near 1.4 GeV is seen to be dominated by the opening of the $K\bar{K}^*$ diffraction threshold. The overall $K\bar{K}^*$ mass distribution is in agreement with the data. Different regions of the $K\bar{K}^*$ effective mass were found to yield differing distributions in t_p, the momentum transfer squared from initial proton to final proton. With the pion diffracting into $K\bar{K}^*$ (or $\bar{K}K^*$) the heavier $K\bar{K}^*$ (or $\bar{K}K^*$) mass states were found to depend less strongly on t_p. In terms of an exponential dependence of this cross section on t_p, i.e., $\exp(b_\pm t_p)$, where $b_\pm$ are the slope parameters for $\pi^\pm p\to(K^+K^-\pi^\pm)p$, we found that $b_\pm$ (as a consequence of the Reggeized Deck amplitude) decreased considerably as the mass $(s_{KK^*})^{1/2}$ increased across the enhancement. The calculated result $b_-(s_{KK^*})>b_+(s_{KK^*})$ agreed quantitatively with the data; it could be explained qualitatively by simply looking at the double Regge diagram. In the diagrammatic representation of the amplitude it is clear that the dominant part of the t_p slope in $\pi^+p\to(\bar{K}^*K^+)p$ is due to the diffractive slope of K^+p scattering. On the other hand, for $\pi^-p\to(K^*K^-)p$ the equivalent portion of the total amplitude is replaced by K^-p scattering which has a much steeper diffractive slope (more absorption) than does K^+p.

The analysis of the Reggeized Deck amplitudes for relative angular momentum between the K and $\bar{K}^*$ indicated a completely dominant $M_L=0$ contribution when the quantization axis was specified by the t-channel helicity frame. This again was the result reported by the experiment.[5] This analysis also yielded cross sections for given $K\bar{K}^*$ partial waves as a function of the $K\bar{K}^*$ effective mass. The S-wave projection for the Regge propagator $R_{\mathrm{I}}\propto s_{KK^*}{}^{\alpha}$ agreed excellently with the data, as did the relative phase between P and S waves. This same calculation yielded a P-wave cross section in the bin, $(s_{KK^*})^{1/2}=1.7\pm0.1$ GeV, which was

roughly 2.5 standard deviations below the experimental result but was in agreement with small values above and below this bin. We feel that this large measured cross section in one bin is the result of the limited statistical accuracy in the experiment; nevertheless, we note that the amount of P wave can be increased by including the direct diagram Fig. 1(c) (which contributes only to this component) in the analysis. (This will not be pursued here.[7]) The higher partial waves are small, and, of these, the largest is the $L=2$ or KK^* D wave, which is completely negligible in the peak region but is ~25% of the total in the tail region at $(s_{KK^*})^{1/2}=2.0$ GeV. We emphasize that this approach to the angular momentum analysis is as straightforward and simple as possible since the $\bar{K}^*$ spin was assumed "averaged" out. But one is not surprised at the good agreement with data in Fig. 8 because of the Stodolsky cancellation arguments.

The possibility that future better data might differentiate between the two forms used for the Regge propagator $R_{\mathrm{I}} \propto s_{KK^*}{}^{\alpha}$ and $R_{\mathrm{II}} \propto [\frac{1}{2}(s_{KK^*}-u)]^{\alpha}$ is of interest. The former gives rise to almost equal amounts of K- and K^*-exchange contributions (see Fig. 6), whereas the latter leads to the K-exchange contribution being nearly twice as large as that due to K^* exchange (see Fig. 2). This difference can be explained by noting that for small-t_π values the Regge trajectory α_{K^*} lies above zero by roughly the amount that α_K is below. Then the ratio

$$[\tfrac{1}{2}(s_{KK^*}-u)]^{\alpha}/s_{KK^*}{}^{\alpha} = [1+(t_\pi - t_p - m_\pi{}^2 - m_K{}^2 - m_{K^*}{}^2)/2s_{KK^*}]^{\alpha}$$

has $t_\pi - t_p - m_\pi{}^2 - m_K{}^2 - m_{K^*}{}^2 < 0$, so for α positive (negative) $d\sigma/ds_{KK^*}$ will be decreased (enhanced). Therefore, a high-statistics experiment which allows deduction of the contribution of the K^*-exchange diagram may well yield fundamental information on dual amplitudes.

Finally, it may become feasible to study the $\bar{K}^{*0}$ interaction. Our calculations show that the pure K-exchange diagram (with or without the direct diagram) cannot explain the (perhaps inadequate) data studied in this paper. This appears to establish convincingly the existence of the vector-$\bar{K}^*$-exchange diagram. Since the pseudoscalar-exchange process is well studied, it would appear that a high-statistics experiment could turn the problem around to deduce the $\bar{K}^*p$ scattering cross section. Also, the kinematical cut on s_{pK^*} discussed in the text gives a good prescription for isolating pure $\bar{K}^*$ exchange. We note further that the cuts on $\cos\theta_{\mathrm{GJ}}$ and ϕ_H include less background from the other diagram when cuts on s_{KK^*} can be simultaneously made; this separation of the contributions becomes better when s_{KK^*} is increased.

Note added. After this work was completed it was pointed out that work by E. Berger and J. Donohue, Phys. Rev. D 15, 790 (1977), suggests that vector-exchange graphs may lead to s-channel helicity conservation. We acknowledge that our analysis of *total* partial-wave information is very approximate; however, the Stodolsky cancellation argument for relative orbital angular momentum information seems to be well illustrated by this reaction as this naive approach agrees well with data. When the exchanges are Reggeized, there seems to be no easy way in this present calculation to cause the vector-exchange $\bar{K}^*$ contribution to dominate over the K-exchange contribution; t-channel helicity conservation therefore results in this particular model calculation.

ACKNOWLEDGMENT

This work was supported by the U. S. Energy Research and Development Administration, Division of Physical Research.

†Address in 1977: Department of Theoretical Physics, University of Oulu, Oulu, Finland.

[1]E.g., G. Ascoli *et al.*, Phys. Rev. D 9, 1963 (1974); G. Ascoli, L. M. Jones, B. Weinstein, and H. W. Wyld, *ibid.* 8, 3894 (1973); G. Fox, in *Experimental Meson Spectroscopy—1972*, proceedings of the Third International Conference, Philadelphia, edited by A. H. Rosenfeld and K.-W. Lai (AIP, New York, 1972), p. 271; R. T. Deck, Phys. Rev. Lett. 13, 169 (1964); U. Maor and T. O'Halloran, Phys. Lett. 15, 281 (1965); L. Stodolsky, Phys. Rev. Lett. 18, 973 (1967).

[2]G. W. Brandenburg *et al.*, Phys. Rev. Lett. 36, 703 (1976).

[3]G. Otter, Aachen University report, 1976 (unpublished).

[4]K. E. Lassila and E. P. Pietiläinen, Lett. Nuovo Cimento 18, 111 (1977); in *Particles and Fields '76*, proceedings of the Brookhaven Meeting of the Division of Particles and Fields of the American Physical Society, edited by H. Gordon and R. F. Peierls (BNL, Upton, New York, 1977), p. H7.

[5]G. Otter *et al.*, Nucl. Phys. B96, 365 (1975).

[6]M. Ross and Y. Y. Yam, Phys. Rev. Lett. 19, 546 (1967).

[7]K. E. Lassila and E. P. Pietiläinen (unpublished). For more discussion of helicity and conservation in the subscattering, see S. Humble, *Introduction to Particle Production in Hadron Physics* (Academic, New York, 1974). Stodolsky's work (see Ref. 1) strongly suggests that the main features of our calculation will not change if λ and λ' are treated differently.

[8]H. Pilkuhn, *Landolt-Bornstein Group 1,* edited by H. Schopper (Springer, Berlin, 1972), Vol. 6, p. 1.
[9]See, e.g., S. U. Chung, R. L. Eisner, N. F. Bali, and D. Lüers, Phys. Rev. 182, 1443 (1969).
[10]J. L. Basdevant and E. L. Berger, Phys. Rev. Lett. 37, 977 (1976).
[11]E. L. Berger, *Three Particle Phase Shift Analysis and Meson Resonance Production, Daresbury Study Series No. 8* (Science Research Council, Daresbury Laboratory, Lancashire, England, 1975), p. 35; Phys. Rev. 166, 1525 (1968).
[12]G. Giacomelli, in *Proceedings of the XVI International Conference on High Energy Physics, Chicago-Batavia, Ill., 1972,* edited by J. D. Jackson and A. Roberts (NAL, Batavia, Ill., 1973), Vol. 3, p. 219; T. Lasinski, R. Levi Setti, B. Schwarzschild, and P. Ukleja, Nucl. Phys. B37, 1 (1972).
[13]J. M. Hammersley and D. C. Handscomb, *Monte Carlo Methods* (Halsted, New York, 1965).
[14]L. Durand, Phys. Rev. 166, 1680 (1968).
[15]J. D. Hansen, G. T. Jones, G. Otter, and G. Rudolph, Nucl. Phys. B81, 403 (1974).
[16]H. H. Seyfert, Techischen Hochschule Aachen dissertation, 1975 (unpublished).